AD-A086 862 AIR FORCE GEOPHYSICS LAB HANSCOM AFB MA F/G 4/2
SHORTRANGE FORECASTING THROUGH EXTRAPOLATION OF SATELLITE IMAGE--ETC(U)
DEC 79 H S MUENCH
UNCLASSIFIED AFGL-TR-79-0294 NL

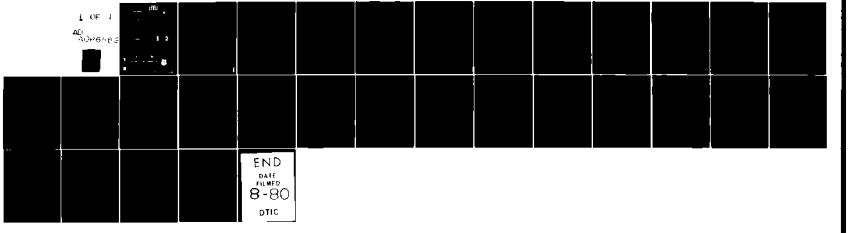

(14) AFGL-TR-79-0294
ERP NO. 685
AFGL-ERP-185

(14) LEVEL III

AD A073 081

(9) Final report

Short-Range Forecasting Through Extrapolation of Satellite Imagery Patterns, Part II: Testing Motion Vector Techniques

(10) H. STUART MUENCH

ADA086862

(11) 14 Dec 79

(12) 30

DTIC
SELECTE
JUL 21 1980
S D
B

(14) (17) 11

AIR FORCE GEOPHYSICS LABORATORY

This report has been reviewed by the ESD Information Office (OI) and is releasable to the National Technical Information Service (NTIS).

This technical report has been reviewed and is approved for publication.

FOR THE COMMANDER

Unclassified

SECURITY CLASSIFICATION OF THIS PAGE (When Data Entered)

REPORT DOCUMENTATION PAGE	READ INSTRUCTIONS BEFORE COMPLETING FORM
1. REPORT NUMBER: AFGL-TR-79-0294	2. GOVT ACCESSION NO.: AD-A086 862
3. RECIPIENT'S CATALOG NUMBER:	
4. TITLE (and Subtitle): SHORT-RANGE FORECASTING THROUGH EXTRAPOLATION OF SATELLITE IMAGERY PATTERNS Part II: Testing Motion Vector Techniques	5. TYPE OF REPORT & PERIOD COVERED: Scientific. Final.
	6. PERFORMING ORG. REPORT NUMBER: ERP No. 685
7. AUTHOR(s): H. Stuart Muench	8. CONTRACT OR GRANT NUMBER(s):
9. PERFORMING ORGANIZATION NAME AND ADDRESS: Air Force Geophysics Laboratory (LYU) Hanscom AFB Massachusetts 01731	10. PROGRAM ELEMENT, PROJECT, TASK AREA & WORK UNIT NUMBERS: 62101F 66700803
11. CONTROLLING OFFICE NAME AND ADDRESS: Air Force Geophysics Laboratory (LYU) Hanscom AFB Massachusetts 01731	12. REPORT DATE: 10 December 1979
	13. NUMBER OF PAGES: 30
14. MONITORING AGENCY NAME & ADDRESS (if different from Controlling Office):	15. SECURITY CLASS. (of this report): Unclassified
	15a. DECLASSIFICATION/DOWNGRADING SCHEDULE:

16. DISTRIBUTION STATEMENT (of this Report)

Approved for public release; distribution unlimited.

17. DISTRIBUTION STATEMENT (of the abstract entered in Block 20, if different from Report)

18. SUPPLEMENTARY NOTES

19. KEY WORDS (Continue on reverse side if necessary and identify by block number)

Short-range forecasting
Satellite meteorology
Cloud motions

20. ABSTRACT (Continue on reverse side if necessary and identify by block number)

An effort is underway at Air Force Geophysics Laboratory to develop automated procedures to make short-range (0-6 hr) terminal weather forecasts using GOES imagery data. A simple approach is to extrapolate the cloud patterns using motion vectors derived from a comparison of successive images. This report describes a test of candidate motion vector techniques using twelve cases of six successive images in a variety of weather conditions. Included in the techniques were two that track brightness centers, three that use cross-covariance, and two using winds aloft. All were

DD FORM 1 JAN 73 1473 EDITION OF 1 NOV 65 IS OBSOLETE

Unclassified

SECURITY CLASSIFICATION OF THIS PAGE (When Data Entered)

20. (Cont)

compared against persistence (no motion, no change). For all time periods and all thresholds, a binary covariance technique had the highest scores but the techniques using winds aloft were very close. Also, no technique was much better than persistence. There is evidence that most (perhaps 75 percent) of the total changes occurring are not due to simple motion of the cloud patterns but due to more complex processes.

Contents

Illustrations

Tables

Short-Range Forecasting Through Extrapolation of Satellite Imagery Patterns

Part II: Testing Motion Vector Techniques

1. INTRODUCTION

The geostationary satellites, transmitting digital data at half-hourly intervals, present meteorologists with a unique opportunity to develop objective short-range forecast techniques. However, the data rates for fine resolution images (1 to 10 km) are very high, requiring computer processing to assist forecasters. At the least, the computer must present data in a form easily and quickly analyzed by the forecaster. A more satisfactory system is to have the computer prepare "guidance" forecasts, automatically, which can be modified by the forecaster when necessary.

In making short-range forecasts, the principal problem is handling meso-scale weather disturbances—patterns with a horizontal scale of 5 to 500 km (3 to 300 miles). In the past, weather data for scales less than 200 km (120 miles) have been very scarce, and the weather satellites with 1 to 5 km resolution have made us aware of the extent to which local weather conditions are associated with the meso-scale circulation patterns (*for example, heavy rains, fog, and stratus*). Our knowledge of synoptic-scale systems (500 km to 5000 km) is quite good, and allows us to successfully forecast the patterns out to at least 36 hr, using any of several techniques, or even simple extrapolation. Largely because of the past lack of data, progress in learning to forecast meso-scale disturbances has been very slow, and our knowledge and forecast ability are perhaps 20 to 40 years behind that for the

(Received for publication 10 December 1979)

larger scales. Dynamic prediction models for meso-scale features are some years in the future, as we do not know the appropriate physics, and computers are lacking in speed and memory to rapidly handle the massive amounts of fine resolution data. Statistical techniques also have problems with fine resolution data in that there are enormous numbers of potential predictors which require an enormous data base for the selection process to ensure reliability on independent data.

This leaves simple extrapolation as a technique which can quickly take advantage of the fine resolution of the satellite data to produce objective forecasts. For many years, radar meteorologists have used the horizontal extrapolation of radar echoes to predict precipitation arrival as well as some severe weather conditions. More recently, the extrapolation technique has been adapted to digital radar output, to automatically produce forecasts.[1] With this technique, one uses two or more successive radar images (5 to 30 min apart) to determine a motion vector that best explains the observed changes in the patterns. The motion vector is then used to look "upstream" on the latest image and deduce the intensity of echoes that will arrive at various time intervals. Finally, one uses algorithms relating radar intensity (or perhaps, echo tops) to surface weather conditions, in a computer program, to automatically produce a fairly detailed short-range forecast.

This approach can be just as easily applied to digital geosynchronous satellite data, and an effort to demonstrate applicability was started at AFGL. The procedure is shown schematically in Figure 1. The first year's progress was reported by Muench and Hawkins[2] and a few points will be reviewed here. A literature search identified several objective techniques for extracting motion vectors from pairs of successive satellite images, and three promising techniques were programmed for the AFGL CDC 6600. The first technique was developed by SRI[3] in 1971 as a means to track individual cloud "clusters" (or groups of high video count) and a version was programmed at AFGL. An updated version of the SRI approach was completed in 1976,[4] and a computer program was assembled based on a FORTRAN listing provided by the Naval Environmental Prediction Research Facility. A third technique, using fast-Fourier transforms (fFt) to obtain cross-covariance, was

1. Austin, G. L., and Bellon, A. (1974) The use of digital radar in short-range forecasting, QJRMS 100:658-664.
2. Muench, H. S., and Hawkins, R. S. (1979) Short-Range Forecasting Through Extrapolation of Satellite Imagery Patterns, Part 1: Motion Vector Techniques, AFGL-TR-79-0096, AD A073308.
3. Endlich, R. M., Wolf, D. G., Hall, D. J., and Brain, A. G. (1971) The use of Pattern recognition techniques for determining cloud motions from sequences of satellite photographs, J. of Appl. Meteor. 10:105-117.
4. Wolf, D. E., Hall, D. J., and Endlich, R. M. (1977) Experiments in automatic cloud tracking using SMS-GOES data, J. of Appl. Meteor. 16:1219-1230.

programmed based on the work of Leese and Novak.[5] Finally, a cross-covariance technique using binary arithmatic was developed and programmed. The four motion vector techniques were tested by using eighteen pairs of "one-mile" resolution satellite images, with the second image being identical to the first except artificially displaced a known amount to simulate a 30-kt (15 m sec^{-1}) motion over a half-hour interval. The overall results of this test are shown in Table 1. Clearly the binary-cross-covariance technique was superior to the other three, with the fFt cross-covariance technique next in accuracy.

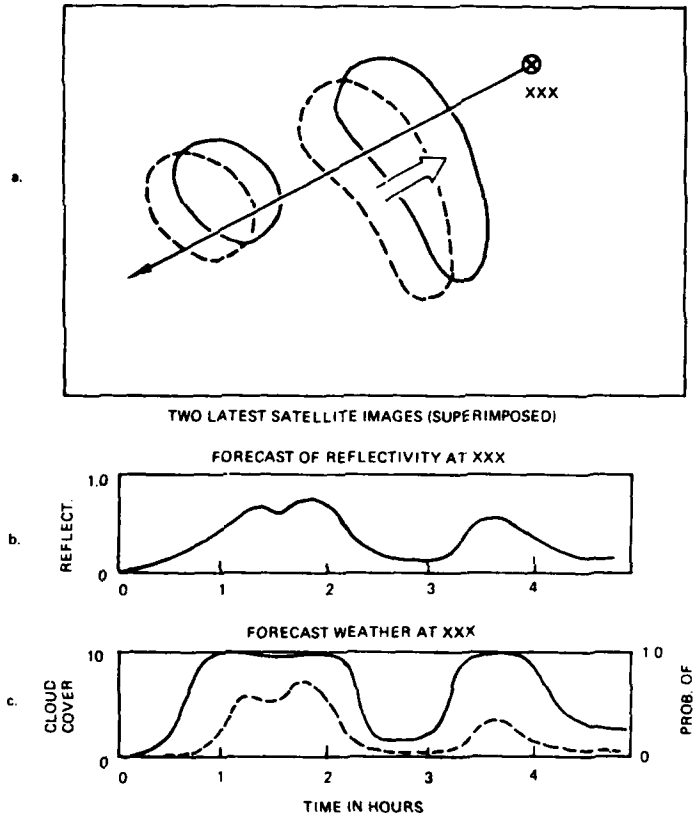

Figure 1. Illustration of Forecasting Through Extrapolation of Satellite Imagery. (a) Derive motion vector, (b) Predict reflectivity by looking "upstream", and (c) Translate forecast reflectivity to surface weather

5. Leese, J.A., and Novak, C.S. (1971) An automated technique for obtaining cloud motion from geosynchronous satellite data using cross-correlation, J. of Appl. Meteor. 10:118-132.

Table 1. Test of Motion Vector Techniques Using Artificial Displacement (18 vectors, simulating 15 m sec^{-1} for 1/2 hr). ϵ_x and ϵ_y are rms errors in 1-mile grid units. Vector error is rms resultant error divided by artificial displacement

	SRI 1971	SRI 1977	fFt Cross-Covariance	Binary Cross-Covariance
ϵ_x	± 8.3	± 6.0	± 4.9	± 0.3
ϵ_y	± 3.9	± 3.7	± 3.8	± 1.5
Vector Error	± 59%	± 49%	± 42%	± 10%

2. PLANS FOR SECOND TEST

The first test was well controlled in that the true motions were predetermined. Further, the test was revealing in that boundary problems were detected with the three least accurate techniques. However, the test was not realistic in that the consecutive images did not include the effects of cloud development and decay as well as the motion. Cloud development would likely cause difficulties and lead to less reliable motion vectors, but further testing would be necessary to determine which technique is least affected. An obvious test would be to use a series of consecutive satellite images to evaluate the performance of each motion vector technique. Unfortunately, with real data there is the question of what is the "true" motion. Some thought was given to having technicians make a determination from images on the McIDAS CRT display, but this procedure did not seem sufficiently objective. Since the motion vectors are to be used in forecasting, a logical answer would be to test the forecast accuracy using the vectors produced by each technique. In decision-making, the simplest way to use a forecast is to proceed with action "A" if the forecast is for less than a threshold, otherwise proceed with action "B". One then evaluates the forecasts by finding which technique produced the most correct forecasts (or decisions), relative to a number of thresholds. So, in this test, series of consecutive satellite images would be used to extract motion vectors, forecasts would be made through simple pattern extrapolation, and the forecasts evaluated by computing correct forecasts relative to several thresholds.

Since the intent is to use the motion vector techniques in automated forecast procedures, we would like the tests to include the wide variety of conditions that occur naturally. The four techniques that were programmed do not have the capability to discriminate snow-cover from clouds and would compute incorrect motion vectors during periods when extensive snow-cover was present in the satellite

image. Thus, much of the winter season data could not be used. Also, there was concern that the half-hourly image rate for GOES would be too infrequent to adequately track convective showers, thus the summer season was excluded. This left the spring and fall seasons as the principal source of data for the tests.

After consideration of such factors as computer capacity, available disc storage, turn-around time, as well as the desire for a thorough test, the test procedure outlined in Figure 2 was adopted and followed. The basic AFGL GOES archive[6] available for the test consists of hourly images during 1977-1978 for the region shown in Figure 3. On three occasions in the spring of 1978, half-hourly images were recorded, and then in October of 1978, half-hourly images were recorded for 4 to 6 hr each workday on a more routine basis. Omitting the period of snow-covered ground, this gave us about 70 days in the fall of 1978 and spring of 1979 for possible tests. On some of these days, scheduled images were missed due to RF interference or hardware failures and days with two or more missing images were rejected, to keep the sample homogeneous. Days when there were insufficient landmarks in view for refined navigation were rejected, as well as days when there were too few clouds (at least 10 percent cloud cover was required). These exclusions narrowed the sample to about 15 days, and from this sample, the 12 cases listed in Table 2 were selected. Each case represents six successive images, normally at half-hourly intervals. In three of the cases there was one interval that was one full hour.

Once a case was selected, a listing of the satellite coordinates of the four weather stations shown in Figure 3 was obtained from the McIDAS system, for each of the six video images. These coordinates were refined by using printouts of 1-mile (1.8 km) resolution data around identifiable landmarks to develop correction factors for each image and provide the best possible estimate for the location of the four stations. At the same time, histograms of the video count were obtained for each image, to compute relative normalization factors for the case. This normalization is based on the assumption that the reflectivity for the 5 percent (95 percent of the pixels are darker) level does not change for the full image (about 600 × 600 miles or 1100 × 1100 km) over the 3-hr period. A normalization factor of 1.00 is assigned to 1700 UT, and the factor usually increased to about 1.10 at three hours to either side.

Next, motion vectors were computed for five different techniques, the same four listed in Table 1 plus another version of the fFt cross-covariance technique (to be described later). The first step was to extract arrays of 1-mile data centered on each of the four stations for six successive images and place the data on the CDC disc "permanent" file. Each motion vector program was executed on the data sets, each computing five successive motion vectors for each location.

6. Muench, H.S., and Keegan, T.J. (1979) Development of Techniques to Specify Cloudiness and Rainfall Rate Using GOES Imagery Data, AFGL-TR-79-0255.

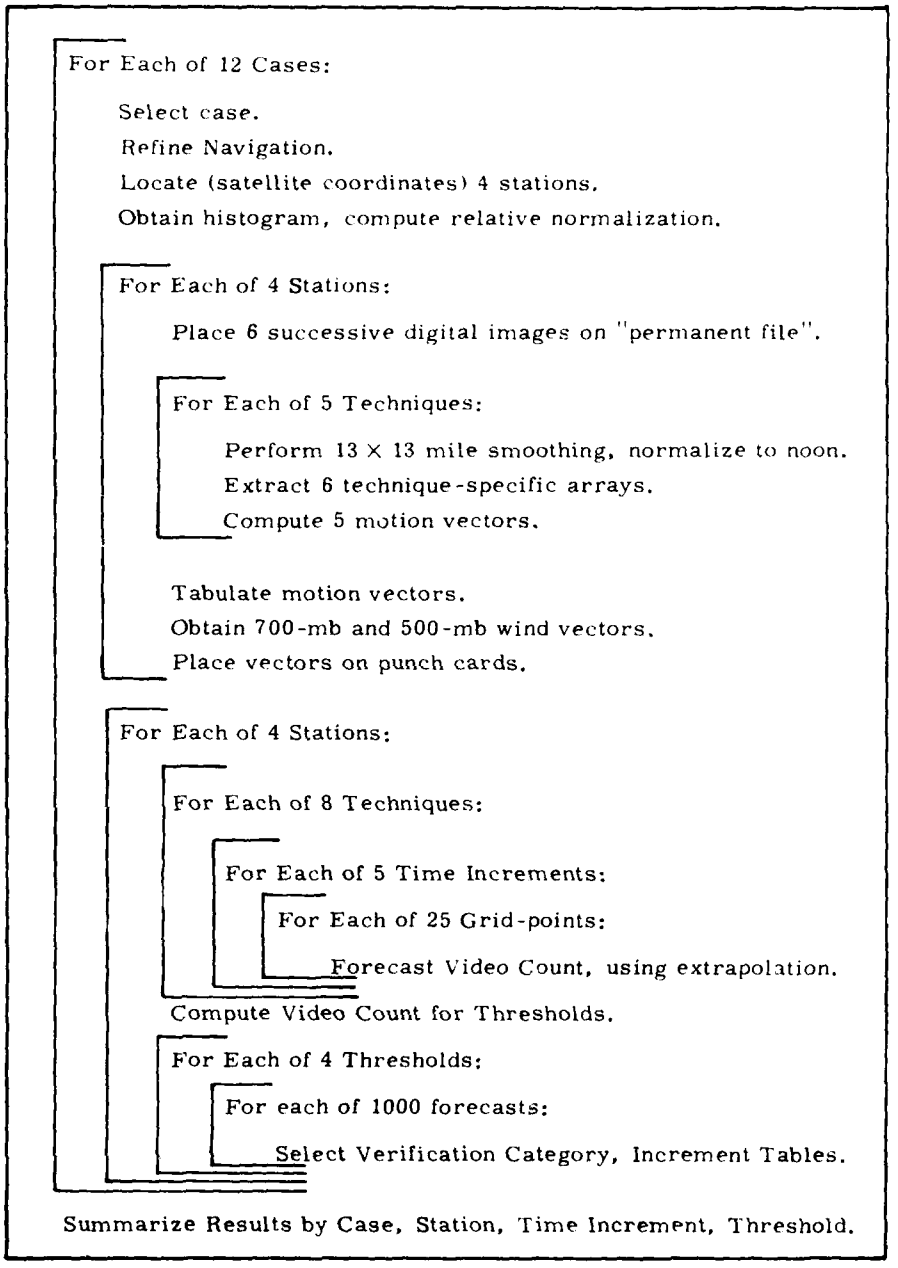

Figure 2. Motion Vector Testing Procedure

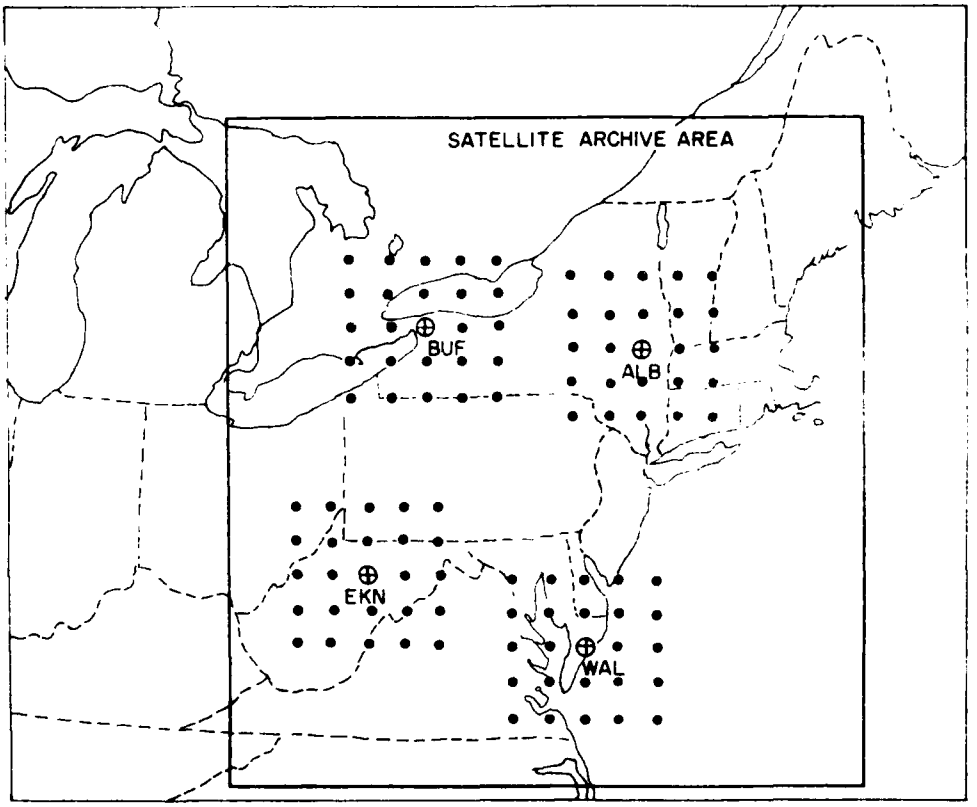

Figure 3. Satellite Data Archive Area and Locations of Grids Used to Verify Motio . ectors

Table 2. Description of Cloud and Synoptic Weather Conditions Associated With Each Test Case

Case	Date	Synoptic Description (1200 UT map)	Prevailing Clouds (1700 UT) by Section ALB	BUF	EKN	WAL
No. 1	14 Nov 78	Occluded front in Great Lakes, SW flow, showers in western NY, PA.	Ac, Sc	Ac-Sc R-	Ac	Ci
Nos. 2, 3	15 Nov 78 a. m., p. m.	Decelerating cold front along East Coast, wave developing in Miss. Valley	Sc	Cs, Sc	Ci, Ac-Sc R-	Ac-Sc
Nos. 4, 5	9 Nov 78 a. m., p. m.	High pressure, radiation for and stratus.	St	St	St	St
Nos. 6, 7	12 May 79 a. m., p. m.	Low in Great Lakes, showers Ont. -E. Tenn., broad southerly flow	Ci-Ac	Ac	Cs, Sc	Ci
Nos. 8, 9	24 Apr 79 a. m., p. m.	High in N. England, broad southerly flow to west, showers Mich. - Ala.	Ci	Cs	Cs, Ac	Ac
No. 10	3 Apr 79	Stationary front along E. Coast, wave in GA.	Ac-Sc	Sc	Ac-Sc RW-	Ac-St
No. 11	26 Mar 79	Deep low in ME, unstable northwest flow to west, widespread "lake" showers.	Ac-Sc	Sc SW-	Sc SW-	Ci, Sc
No. 12	20 Dec 78	High over N. England, deepening low ILL., precip. spreading east into PA.	Ac/As	Ac/As	Ac-St R	Ci, Ac

/ denotes mixed types

- denotes merging in vertical

, denotes distinct layers

This test provided an opportunity to evaluate three additional techniques used by meteorologists to serve as controls. First, there is the 700-mb wind, often used to extrapolate radar patterns; second, there is half of the 500-mb wind, often used to extrapolate short-wave weather patterns; and third, there is persistence, meaning no change with time, equivalent to no motion—an effective technique in the zero to 3-hr forecast period. So, to the five computed motion vectors, we added the 700-mb wind, one-half the 500-mb wind, and a zero-speed vector (for persistence). At the stations ALB, BUF, and WAL the 1200 UT radiosonde winds were used, and at EKN an interpolated wind was used, based on data from Pittsburgh, Pennsylvania and Dulles Airport, Virginia.

Once the motion vectors were computed and assembled, the next task was to compute the extrapolation forecasts and the verifications. At each of the four stations shown in Figure 3, a 5 × 5 grid was located with a 36-mile (64-km) separation. For each technique, each image and each grid-point, a vector was extended "upwind", as indicated in Figure 1, distances to represent motion over 1/2, 1, 1-1/2, 2, and 2-1/2 hours. A forecast of the digital count was made for each of the time intervals by averaging the four nearest 1-mile resolution satellite values. Since the navigation is only accurate to about ± 2 to 4 miles (± 4-7 km), a more precise interpolation is not justified. The video count values had been normalized to noon of that day by using the factor described earlier.

While we could use the six consecutive images to extract five motion vectors using images 1/2 hr apart, there was no point in making forecasts out to 2-1/2 hr from each motion vector as the verification data were not necessarily in the six-image data file. Table 3 lists the image times used in one case to extract the motion vectors and to make forecasts and perform a verification. In this case, there were no forecasts and no verifications beyond 2 hr, but in a few cases there was a 1-hr interval between images among the normal 1/2-hr intervals and forecasts and verifications were made out to 2-1/2 hours.

Table 3. Example of Motion Vectors and Forecasts From Six Consecutive Satellite Images

Motion Vectors	Forecasts (Initial time-Verification time)				
Image Pair	1/2 hr*	1/2 hr	1 hr	1-1/2 hr	2 hr
1500-1530:	1500-1530	1530-1600	1530-1630	1530-1700	1530-1730
1530-1600:	1530-1600	1600-1630	1600-1700	1600-1730	
1600-1630:	1600-1630	1630-1700	1630-1730		
1630-1700:	1630-1700	1700-1730			
1700-1730	1700-1730				

*dependent data forecast

Before starting the verifications of the forecasts, the noontime (1700 UT) video counts for reflectivities of 0.30, 0.55, 0.75, and 0.90 were found in order to serve as thresholds. These counts were extracted from tables of normalization based on a procedure described by Muench and Keegan.[6] This normalization served to insure compatibility between cases months apart in time, while the normalization based on the histograms for a specific case largely eliminated incompatibility between images from hour to hour due to changing sun angle.

The remainder of the computer program for forecasting and verification examined each forecast video count and the associated video count observed at verification time to see which of four conditions it satisfied with respect to a threshold as indicated schematically in Figure 4. These 2 × 2 contingency tables were developed separately for each station, each forecast interval, and each threshold. These data were stored and summed over all 12 cases. Percent correct scores were computed using the relation shown at the bottom of Figure 4, and skill scores relative to persistence were computed by:

$$\text{Skill Score} = \frac{\text{Percent Correct} - \text{Persistence Percent Correct}}{1.0 - \text{Persistence Percent Correct}}$$

Overall results are shown in Table 4.

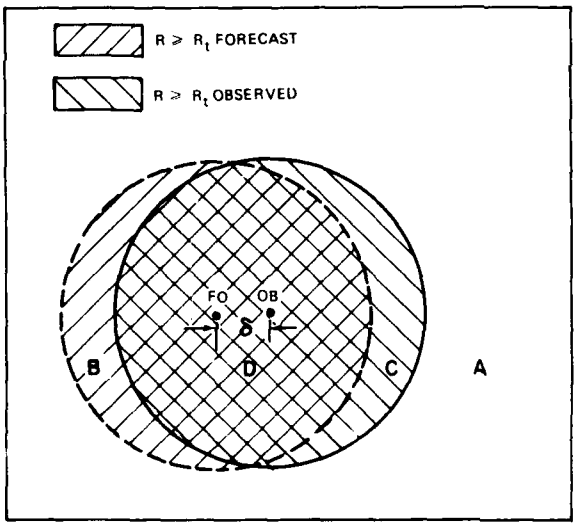

OBSERVED \ FORECAST	< R_t	≥ R_t
< R_t	A	B
≥ R_t	C	D

δ = MOTION ERROR

PERSISTENCE

δ = S (SPEED) · Δt

MOTION VECTOR TECHNIQUE

δ = ε · S · Δt

PERCENT CORRECT = P = (A + D) / (A + B + C + D)

Figure 4. Illustration of Forecast Errors Due to Motion Vector Frrors. (Simple motion, *no development*)

Table 4. Percent Correct and Skill Score for Forecast Techniques. Twelve cases, all times and all thresholds combined, 2 · 2-mile area

	SRI 1977	SRI-AFGL 1971	fFt Cross-Covariance 1	fFt Cross-Covariance 2	Barnes Cross-Covariance
Percent Correct	0.892	0.880	0.897	0.900	0.903
Skill Score	-0.05	-0.16	0.00	0.03	0.06

	700-mb Wind	$\frac{1}{2}$ 500-mb Wind	Persistence
Percent Correct	0.900	0.898	0.897
Skill Score	0.03	0.01	0.00

3. RESULTS

The relative skill of the five motion vector techniques is consistent in this test with the order found in the artificial displacement test (Table 1), with the Barnes technique first, followed by the two fFt techniques and the SRI techniques last. The newer version of the fFt that was added (labelled No. 1 in Table 3) was another attempt to solve a boundary problem, this time by using a 48 × 48 initial array and a 32 × 32 final array. While early trials were encouraging, the contractor responsible for the fFt program cautioned that aliasing might cause erratic behavior. The results here suggest this version is no better, perhaps a little worse than the earlier version (fFt No. 2). Considering that there were large differences in motion vector accuracy between techniques in the first test (Table 1), the differences in percent correct shown in Table 4 are remarkably small.

The results obtained for the three control techniques (two radiosonde winds and persistence) are shown at the bottom of Table 4. Perhaps surprising, these controls scored quite high. The two techniques requiring radiosonde winds scored almost as high as the covariance techniques. This raises a question whether it is worth the computational effort to obtain a covariance-based motion vector when a relatively easily obtained radiosonde winds would do as well (at least where radiosonde winds are available). Furthermore, none of the techniques was much better than persistence, which is readily apparent by examining the skill scores relative to persistence. In fact, some skill scores are negative! This is a rather disturbing result. The figures indicate that in all forecasts, only about 10 percent of the time was a threshold crossed, and only one of sixteen threshold crossings was

successfully forecast by the best of the techniques.

Figure 5 shows the percent correct for each technique, for each of four thresholds, and Figure 6 shows percent correct for each of the five forecast intervals. The relative standings of the techniques is essentially the same, regardless of threshold or forecast interval, lending confidence to the results. One notes the highest score are for the highest threshold, but this can be misleading. Values above the highest threshold are very infrequent, and the high scores come not by correct forecasts of their occurrence, but rather by the correct forecast of their non-occurrence (area A in Figure 4). In Figure 6, the overall level of percent correct drops almost monotonically as the forecast time interval increases, as one might expect.

When the results of the forecast verification program indicated that the techniques were scarcely any better than persistence, the first impression was one of disbelief, and there were worries of programming or navigation errors causing this result. The computer program was carefully inspected, revealing a 1/2-grid-length round-off error in forecast vectors we well as a logical error in handling missing data. However, when the program was corrected and the data rerun, only trivial differences resulted. In addition, data listings for the areas around Buffalo and Wallops Island showed stable locations of the coast lines relative to the center of the grid, evidence that the navigation was reliable.

Another possible cause of the low skill scores was thought to be due to the 2 × 2 pixel average used in the forecasts and verifications. From experience with small-scale weather systems, one would not expect clouds or cells as small as 2 miles in diameter to have a lifetime as long as 1/2 to 2-1/2 hours. Even if they had sufficient lifetime, extreme accuracy in the motion vector would be necessary to pinpoint future positions if they were moving at even a moderate speed such as 30 kts (15 m sec^{-1}). So, the forecast-verification procedure was repeated, but this time using video data that were smoothed over 8 rows and 16 elements, equivalent to a 13 × 13 mile (23 × 23 km) smoothing. While the details of this verification can be found in Appendix A, the percent correct for persistence and the binary cross-covariance technique are shown in Figure 7, along with comparable results for the 2 × 2 pixel average. The smoothing obviously had but little effect on the relative scores, though the binary technique score improves more than persistence at 2 hr and improves less at 1/2 hour. The most noticeable effect is that all scores were higher for the smoothed image data, as one would expect if the smaller sized features were more short-lived.

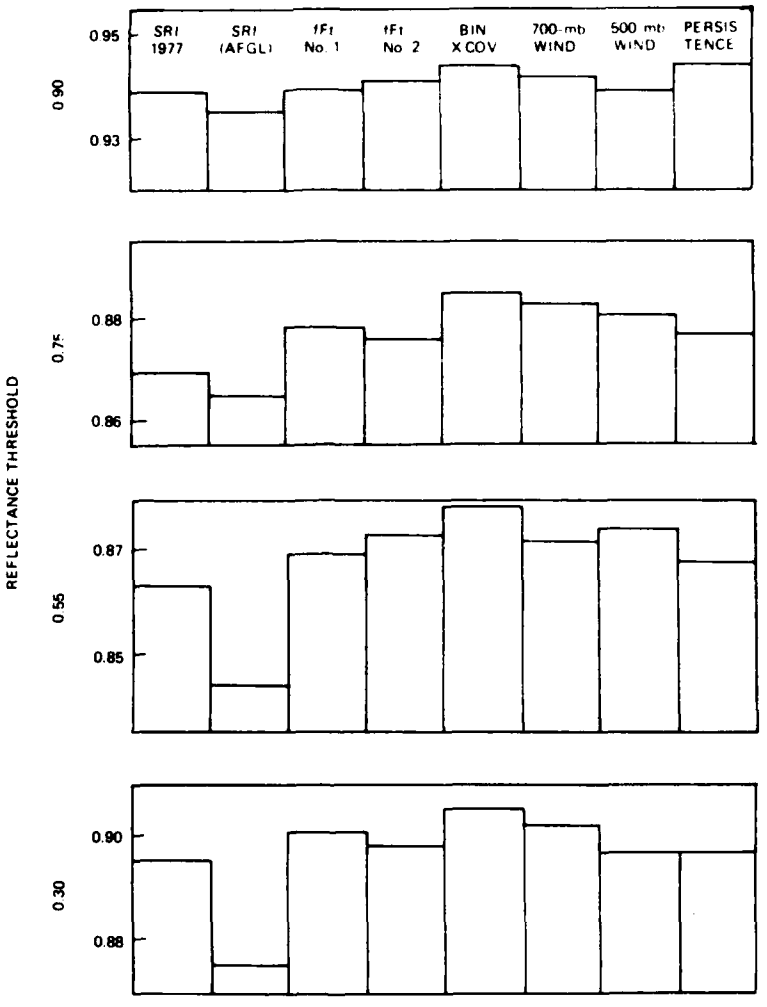

Figure 5. Percent Correct for Displacement Forecasts, by Threshold. Verification for 2 × 2 mile area (5-time intervals combined)

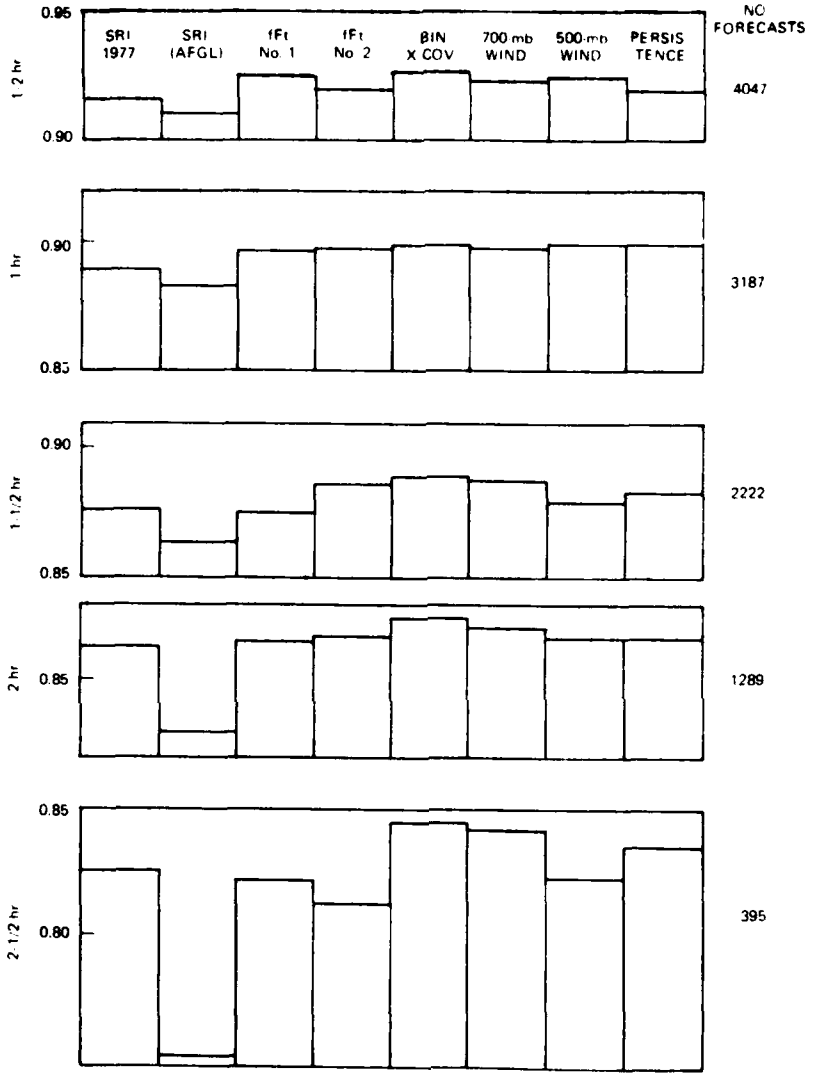

Figure 6. Percent Correct for Displacement Forecasts, by Time Interval. Verification for 2 × 2-mile area (4 Thresholds combined)

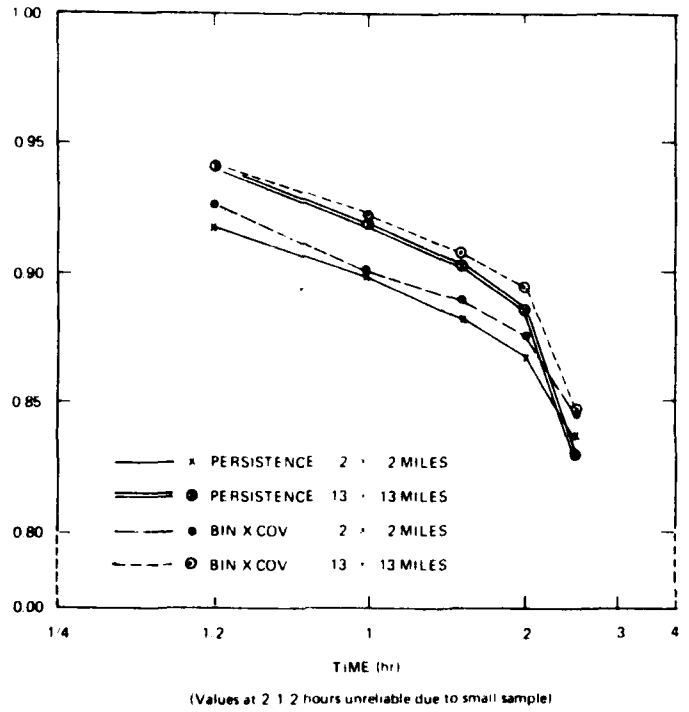

Figure 7. Percent Correct for Displacement Forecasts vs Log of Time Interval, 2 × 2-mile area and 13 × 13-mile area

At this point we should stop and ask how much improvement over persistence should we realistically expect. If we look back at Figure 4, we see that for a given displacement error δ there will be a specific correct forecast (areas A and C). If we define δ as the actual displacement—the speed times the time interval—then we will have the percent correct score for persistence, which assumes no motion. For any other motion vector technique, we define the displacement error as $\epsilon\,\delta$. In the artificial displacement tests[2] ϵ ranged from ± 0.59 down to ± 0.10 for the binary covariance technique. Now, if the speed of the pattern is constant, we see that the displacement error for a motion vector technique will be identical to that of persistence if the time interval for the motion vector technique is $1/\epsilon$ times the time interval for persistence. Thus, the percent correct for the binary covariance technique with ϵ = 0.10 for a 5-hr forecast interval should be the same as persistence for a 1/2-hr interval, provided the observed change in the pattern was due only to simple horizontal motion.

When looking at successive motion vectors for a case, it was obvious that the "noise level" in the vectors was much greater than 10 percent. If the mean of five successive vectors is assumed to be the "true" vector, then, an average departure for the binary covariance motions was about 50 percent of the speed. This indicates that we should expect the percent correct score at 2 hr to be equivalent to persistence at 1 hour. In fact, the results are not that good, in that persistence at 1 hr was 0.899 while the binary covariance at 2 hr was only 0.874. Persistence at 2 hr was 0.867, so the improvement over persistence was only 0.007 instead of an expected improvement of 0.032. When the verification was performed with the smoothed data, the binary covariance score at 2 hr was 0.893 and persistence at 1 hr was 0.918 and at 2 hr was 0.884, so the improvement was only 0.009 instead of an expected 0.034. In the first verification, only 22 percent of the expected gain was achieved (0.007/0.032) and in verification with smoothed data only 26 percent was achieved.

Not all cases were alike, and there were 17 instances when ϵ for one of the four stations was less than 0.25. For this sample, the binary cross-covariance score at 2 hr should have been as high as persistence at 1/2 hour. However, again the scores were lower, and the improvement over persistence was only 25 percent of what might be expected. Considering these results alone, there is strong evidence that most of the changes (perhaps 75 percent) in the patterns are due to causes other than simple horizontal motion. Further, this conclusion is not altered by increasing the horizontal smoothing from 2 miles (3.6 km) to 13 miles (23 km). This apparent complex behavior of the video patterns complicates the forecast procedure in two ways. First, the task of determining a motion vector is made more difficult, as evidenced by the increase in uncertainty for the binary covariance technique from 0.10 for artificial displacement to 0.25 for the most stable cases to 0.50 for all cases. Second, even with good motion vectors only a small portion (about 25 percent) of the gain over persistence can be achieved.

The low skill scores of simple extrapolation are familiar to those who worked with the AFGL Mesonet experiment. Chisholm[7] developed objective techniques to extrapolate patterns of low visibility (scale size 10 to 40 km) and found "—improvement in sensor-equivalent-visibility forecast skill of between 10 and 20 percent over a single station conditional climatology model for forecast intervals ranging from 15 to 60 minutes". Muench and Brown[8] noted "—we do find time

7. Chisholm, D.A. (1976) Objective Prediction of Mesoscale Variations of Sensor Equivalent Visibility During Advective Situations, AFGL-TR-76-0132, AD A030332.

8. Muench, H.S., and Brown, H.A. (1977) Measurements of Visibility and Radar Reflectivity During Snowstorms in the AFGL Mesonet, AFGL-TR-77-0148, AD A049258.

periods when simple translation with speed of about 15 m sec^{-1} is taking place; we also find many times periods when large oscillations (periods of an hour or more) in both extinction coefficient and radar return take place, but which cannot be explained as simple translation".

4. SUMMARY AND CONCLUSIONS

Confirming earlier tests, the binary cross-covariance technique has the highest score of the several techniques tested with successive GOES image, regardless of the time interval of forecast or the verification threshold. However, the scores were only slightly better than those using motion vectors derived from radiosonde winds and those based on persistence. That the binary technique scored better than two versions of the fFt covariance routines does not reflect any inherent advantage but only that it is simpler to program and more quickly refined. Any or all of the techniques used in this study could probably be refined, and recent communications[9] indicated that an update of the SRI model had been made and is available for testing.

At this point it appears that the pursuit of better motion vectors is not likely to be very rewarding in terms of improved forecasting, as most (perhaps 75 per cent) of the change in cloud reflectivity at a given location appear to be due to processes other than simple motion of the pattern. A fresh approach seem to be called for, perhaps examining cases to isolate the sources of the complexities in the observed cloud behavior. For example, the imagery data often contain clouds at different altitudes and as such are subject to different motion fields. Information from the GOES infrared channel may be able to separate the layers, making independent tracking and forecasting possible. There also may be a mix of moving and stationary waves, stationary waves associated with topography, some waves generated by and moving with synoptic-scale flow patterns and some gravity waves.[10] With appropriate temporal and spatial filtering, these waves may be identified and forecast.

Both researchers and operational forecasters alike have long been frustrated in their efforts to produce forecasts better than persistence for the 0 to 3-hr time interval. While these tests of motion vector techniques using simple extrapolation have shown similar results, the resolution and frequency of GOES observations should provide the means to identify the causes of the complex behavior and lead to improved forecasts.

---

9. Private communication, (July, 1979).
10. Eom, K. J. (1975) Analysis of the gravity wave occurrence of 19 April 1970 in the midwest, Mo. Wea Rev. 103:217-226.

References

1. Austin, G.L., and Bellon, A. (1974) The use of digital radar in short-range forecasting, QJRMS 100:658-664.
2. Muench, H.S., and Hawkins, R.S. (1979) Short-Range Forecasting Through Extrapolation of Satellite Imagery Patterns, Part 1: Motion Vector Techniques, AFGL-TR-79-0096, AD A073308.
3. Endlich, R.M., Wolf, D.G., Hall, D.J., and Brain, A.G. (1971) The use of pattern recognition techniques for determining cloud motions from sequences of satellite photographs, J. of Appl. Meteor. 10:105-117.
4. Wolf, D.E., Hall, D.J., and Endlich, R.M. (1977) Experiments in automatic cloud tracking using SMS-GOES data, J. of Appl. Meteor. 16:1219-1230.
5. Leese, J.A., and Novak, C.S. (1971) An automated technique for obtaining cloud motion from geosynchronous satellite data using cross-correlation, J. of Appl. Meteor. 10:118-132.
6. Muench, H.S., and Keegan, T.J. (1979) Development of Techniques to Specify Cloudiness and Rainfall Rate Using GOES Imagery Data, AFGL-TR-79-0255.
7. Chisholm, D.A. (1976) Objective Prediction of Mesoscale Variations of Sensor Equivalent Visibility During Advective Situations, AFGL-TR-76-0132, AD A030332.
8. Muench, H.S., and Brown, H.A. (1977) Measurements of Visibility and Radar Reflectivity During Snowstorms in the AFGL Mesonet, AFGL-TR-77-0148, AD A049258.
9. Private communication, (July, 1979).
10. Eom, K.J. (1975) Analysis of the gravity wave occurrence of 19 April 1970 in the midwest, Mo. Wea Rev. 103:217-226.

Appendix A

Tables of Scores by Time Interval, Threshold, Verification Area, and Section (Station)

Table A1. Percent Correct for 12 Cases, 2 × 2-Mile Area, by Time Interval and Threshold

Technique	Time Interval in Hours							All Time Intervals Reflectivity Threshold			
	-0.5	0.5	1.0	1.5	2.0	2.5	All	0.30	0.55	0.75	0.90
SRI 1977	0.915	0.916	0.890	0.877	0.863	0.826	0.892	0.845	0.863	0.869	0.939
SRI 1971 (AFGL prog)	0.911	0.910	0.883	0.863	0.830	0.751	0.880	0.874	0.844	0.865	0.935
fFt-1 (2 sizes)	0.921	0.923	0.897	0.875	0.865	0.822	0.897	0.901	0.869	0.878	0.939
fFt-2 (no slope)	0.920	0.919	0.898	0.887	0.867	0.812	0.900	0.898	0.873	0.876	0.941
Binary X covariance	0.922	0.926	0.898	0.889	0.874	0.844	0.903	0.905	0.878	0.885	0.944
700-mb Wind	0.920	0.922	0.898	0.888	0.870	0.871	0.900	0.902	0.872	0.883	0.942
1/2 500-mb Wind	0.921	0.923	0.899	0.879	0.867	0.822	0.898	0.897	0.874	0.881	0.939
Persistence	0.918	0.918	0.899	0.882	0.867	0.835	0.897	0.897	0.868	0.877	0.944
No. Forecasts	5072	4047	3187	2222	1289	395	11140	11140	11140	11140	11140

Table A2. Percent Correct for 12 Cases, 13 × 13-Mile Area, by Time Interval and Threshold

Technique	Time Interval in Hours							All Time Intervals Reflectivity Threshold			
	-0.5	0.5	1.0	1.5	2.0	2.5	All	0.30	0.55	0.75	0.90
SRI 1977	0.938	0.937	0.912	0.895	0.887	0.832	0.912	0.907	0.892	0.880	0.968
SRI 1971 (AFGL prog)	0.929	0.931	0.896	0.880	0.857	0.803	0.899	0.891	0.867	0.874	0.965
fFt-1 (2 sizes)	0.940	0.940	0.912	0.890	0.885	0.825	0.913	0.911	0.884	0.887	0.968
fFt-2 (no slope)	0.939	0.938	0.912	0.896	0.888	0.821	0.912	0.910	0.892	0.879	0.969
Binary X covariance	0.942	0.940	0.919	0.904	0.893	0.844	0.919	0.915	0.898	0.892	0.970
700-mb Wind	0.942	0.942	0.918	0.903	0.888	0.856	0.919	0.922	0.894	0.893	0.967
1/2 500-mb Wind	0.939	0.938	0.915	0.902	0.895	0.848	0.917	0.914	0.898	0.891	0.865
Persistence	0.941	0.940	0.918	0.901	0.884	0.828	0.915	0.915	0.892	0.882	0.972
No. Forecasts	5077	4052	3197	2227	1289	395	11160	11160	11160	11160	11160

Table A3. Skill Score Relative to Persistence, for 12 Cases, 2 × 2-Mile Area, by Time Interval and Threshold

Technique	Time Interval						Reflectance Threshold (All Times)			
	0.5	1.0	1.5	2.0	2.5	All	0.30	0.55	0.75	0.90
SRI-77	-0.02	-0.05	-0.04	-0.03	-0.06	-0.05	-0.02	-0.04	-0.06	-0.09
SRI-AFGL	-0.10	-0.16	-0.16	-0.28	-0.51	-0.16	-0.22	-0.18	-0.10	-0.16
fFt No. 1	+0.06	-0.02	-0.06	-0.02	-0.08	+0.00	+0.04	+0.01	+0.01	-0.09
fFt No. 2	+0.01	-0.01	+0.04	+0.00	-0.14	+0.03	+0.01	+0.04	-0.01	-0.05
BIN X COV	+0.10	+0.00	+0.06	+0.05	+0.06	+0.06	+0.08	+0.08	+0.06	+0.00
700-mb Wind	+0.05	-0.01	+0.05	+0.02	+0.04	+0.04	+0.05	+0.03	+0.05	-0.04
500-mb Wind	+0.06	+0.00	-0.02	+0.00	-0.08	+0.01	+0.00	+0.04	+0.03	-0.09
No. Forecasts	4047	3187	2222	1289	395	11140	11140	11140	11140	11140

Table A4. Skill Score Relative to Persistence, for 12 Cases, 13 × 13-Mile Area, by Time Interval and Threshold

Technique	Time Interval						Reflectance Threshold (All Times)			
	0.5	1.0	1.5	2.0	2.5	All	0.30	0.55	0.75	0.90
SRI-77	-0.05	-0.07	-0.06	+0.03	+0.02	-0.04	-0.09	+0.00	-0.02	-0.14
SRI-AFGL	-0.15	-0.27	-0.21	-0.23	-0.14	-0.19	-0.28	-0.23	-0.07	-0.25
fFt No. 1	+0.00	-0.07	-0.11	+0.01	-0.02	-0.02	-0.05	-0.07	+0.04	+0.14
fFt No. 2	-0.03	-0.07	-0.05	+0.03	-0.04	-0.04	-0.06	+0.00	-0.02	-0.11
BIN X COV	+0.00	+0.01	+0.03	+0.08	+0.09	+0.05	+0.00	+0.06	+0.08	-0.07
700-mb Wind	+0.03	+0.00	+0.02	+0.03	+0.16	+0.05	+0.08	+0.02	+0.09	-0.18
500-mb Wind	-0.03	-0.04	+0.01	+0.10	+0.12	+0.02	-0.01	+0.06	+0.08	-0.29
No. Forecasts	4052	3197	2227	1199	395	11160	11160	11160	11160	11160

Table A5. Percent Correct for 12 Cases, All Intervals and All Thresholds Combined, by Sections (Stations)

		SRI 77	SRI AFGL	fFt No. 1	fFt No. 2	BIN X COV	700-mb Wind	500-mb Wind	Persistence
2 × 2 Mi.	BUF	0.886	0.876	0.846	0.893	0.902	0.899	0.907	0.896
	ALB	0.901	0.875	0.895	0.897	0.897	0.900	0.896	0.901
	EKN	0.866	0.862	0.883	0.880	0.889	0.877	0.872	0.876
	WAL	0.914	0.904	0.911	0.917	0.921	0.921	0.917	0.914
	ALL	0.892	0.880	0.897	0.900	0.903	0.900	0.898	0.897
13 × 13 Mi.	BUF	0.909	0.897	0.918	0.915	0.921	0.925	0.928	0.915
	ALB	0.917	0.898	0.907	0.912	0.916	0.912	0.914	0.919
	EKN	0.893	0.885	0.906	0.902	0.914	0.904	0.895	0.897
	WAL	0.929	0.915	0.919	0.925	0.924	0.933	0.930	0.930
	ALL	0.912	0.899	0.913	0.912	0.919	0.919	0.917	0.915